Wind and Structures, Vol. 7, No. 1 (2004) 55-70
DOI: http://dx.doi.org/10.12989/was.2004.7.1.055

Advanced aerostatic stability analysis of suspension bridges

Ru-Cheng Xiao† and Jin Cheng‡

Department of Bridge Engineering, Tongji University, Shanghai, 200092, China
(Received August 28, 2003, Accepted January 26, 2004)

Abstract. Aerostatic instability of a suspension bridge may suddenly appears when the deformed shape of the structure produces an increase in the value of the three components of displacement-dependent wind loads distributed in the structure. This paper investigates the aerostatic stability of suspension bridges using an advanced nonlinear method based on the concept of limit point instability. Particular attention is devoted to aerostatic stability analysis of symmetrical suspension bridges. A long-span symmetrical suspension bridge (Hu Men Bridge) with a main span of 888 m is chosen for analysis. It is found that the initial configuration (symmetry or asymmetry) may affect the instability configuration of structure. A finite element software for the nonlinear aerostatic stability analysis of cable-supported bridges (NASAB) is presented and discussed. The aerostatic failure mechanism of suspension bridges is also explained by tracing aerostatic instability path.

Keywords: suspension bridges; aerostatic stability; three components of displacement-dependent wind loads; geometric nonlinearity; aerostatic failure mechanism

1. Introduction

For slender suspension bridges, wind stability can be classified into two categories according to the wind loads acting on a bridge: aerodynamic stability and aerostatic stability. Most research works on wind stability of suspension bridges mainly focus on aerodynamic stability (Agar 1988, 1989, Honda, *et al.* 1998, Boonyapinyo, *et al.* 1999, Xu, *et al.* 2000). Attention to the aerostatic stability of suspension bridges was relatively less, probably because the flutter onset wind velocity is generally much lower than the critical wind velocity under static wind loads for suspension bridges. However, with the increasing central span length of suspension bridges, suspension bridges become very slender and light in weight, which increases the sensitivity of the bridge response to static wind loads. On the other hand, experimental observations suggest that the aerostatic instability of suspension bridges can occur under the action of static wind loads (Hirai, *et al.* 1967). Therefore, investigation on the aerostatic stability of suspension bridges is of considerable importance.

Aerostatic instability can be categorized into two types according to modes of static instability: torsional divergence and lateral-torsional buckling. The detailed description of the two phenomena of aerostatic instability can be found in Boonyapinyo, *et al.* (1994). Simiu and Scanlan (1978) proposed a linear method to analyze the torsional divergence of long span bridges. Xiang, *et al.*

† Professor
‡ Assistant Research Professor

(1996) rewrote their method by introducing first symmetric torsion frequency. However, the above two methods were all based on assumptions of a linearized derivative of pitch moment as well as linear structural stiffness matrix; the nonlinear effects arising from bridge structure and the three components of wind load were not considered. Therefore, the critical wind velocity causing aerostatic instability cannot be accurately calculated, the mode of instability as well as the coupling effect cannot be considered, and the wind velocity-deformation path of the bridge from applied wind velocity to divergence cannot be traced. Boonyapinyo, *et al*. (1994) proposed a nonlinear method that combines eigenvalue analysis and updated bound algorithms to investigate the aerostatic stability of cable-stayed bridges. However, their algorithm requires the calculation of critical wind velocity to be begun from applying initial wind velocity, leading to considerable computer time in prediction the instability wind velocity of cable-stayed bridges. More importantly, their algorithm is based on the bifurcation point instability concept. As indicated in Cheng, *et al*. (2002), the concept of bifurcation point instability based on the eigenvalue analysis will be invalid for suspension or cable-stayed bridges. Therefore, the nonlinear method based on the bifurcation point instability concept is inappropriate for the aerostatic stability analysis of suspension bridges. Hence, there is a need for a nonlinear method based on the concept of limit point instability to analyze the aerostatic stability of suspension bridges. Recently, Cheng, *et al*. (2002) proposed a nonlinear method to analyze aerostatic stability of suspension bridges. This method is based on the concept of limit point instability. Moreover, the method has the advantage of reducing the computing time dramatically. This is because that the step-by-step applying wind velocity process in the traditional nonlinear method is not required. Therefore, this method is employed for the aerostatic stability analysis in this paper.

Commercial finite element programs used in civil engineering today cannot be readily used for the aerostatic stability analysis of cable-supported bridges as they lack some capabilities like the calculation of displacement-dependent wind loads, the prediction of critical wind velocity and determination of initial configurations of cable-supported bridges. On the other hand, to the authors knowledge, study on aerostatic failure mechanism of suspension bridges has not been reported in the literature. However, as bridge engineers increasingly consider aerostatic stability of suspension bridges and central span length of suspension bridges becomes longer, investigation on the aerostatic failure mechanism of suspension bridges becomes especially important to be able to accurately understand the aerostatic behavior of suspension bridges.

The aims of this paper is to further investigate the aerostatic stability of suspension bridges, to present a fully interactive software for the Nonlinear Aerostatic Stability Analysis of cable-supported Bridges, NASAB and to explain the aerostatic failure mechanism of suspension bridges by tracing aerostatic instability path. It should be pointed out that the example bridge used in this paper is the Hu Men suspension bridge with a 888 m-long center span, which is one of the longest central span suspension bridge in China. Different from the example bridge (Jiang Yin suspension bridge) used in Cheng, *et al*. (2002), the Hu Men suspension bridge is symmetrical with respect to the midspan of the bridge.

2. Three components of wind loads

The three components of wind load are drag force, lift force and pitch moment. Consider a section of bridge deck in a smooth flow, as shown in Fig. 1. Assuming that under the effect of the mean wind velocity V with the angle of incidence α_0, the torsional displacement of deck is θ. Then

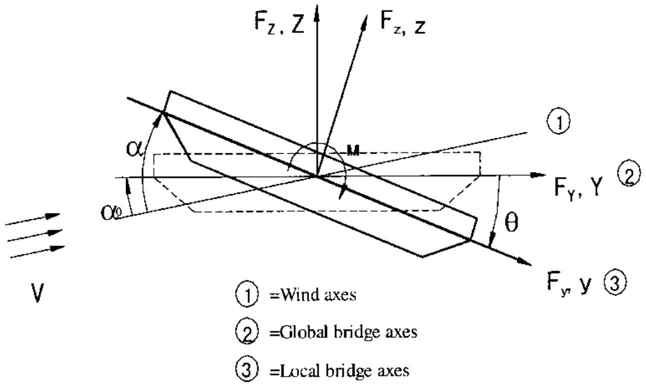

Fig. 1 Motion of Bridge deck and three components of wind loads in different axes

the effective wind angle of attack is $\alpha = \alpha_0 + \theta$. The components of wind forces per unit span acting on the deformed deck can be written in wind axes as

$$\text{Drag force:} \quad F_y(\alpha) = \frac{1}{2}\rho V^2 C_y(\alpha) D \tag{1a}$$

$$\text{Lift force:} \quad F_z(\alpha) = \frac{1}{2}\rho V^2 C_z(\alpha) B \tag{1b}$$

$$\text{Pitch moment:} \quad M(\alpha) = \frac{1}{2}\rho V^2 C_M(\alpha) B^2 \tag{1c}$$

Where $C_y(\alpha)$, $C_z(\alpha)$ and $C_M(\alpha)$=the coefficients of drag force, lift force, and pitch moment in local bridge axes, respectively; B=bridge width; D=the vertical projected area.

The wind forces in Eq. (1) are the function of the torsional displacement of structure. They vary as the girder displaces. Therefore, the three components of wind load are displacement dependent.

3. Method of nonlinear analysis

A detailed description of the nonlinear analysis method used in this paper is presented in Cheng (2000). For this reason, this section provides only a brief summary of this description.

The nonlinear incremental equilibrium equation under the three components of displacement-dependent wind loads may be written as:

$$[K(u)] \cdot \{u\} = P(F_y(\alpha),\ F_z(\alpha),\ M(\alpha)) \tag{2}$$

where $[K(u)]$=the structural stiffness matrix including elastic stiffness matrix and geometrical stiffness matrix; $\{u\}$=the nodal displacement vector; $P(F_y(\alpha), F_z(\alpha), M(\alpha))$=the total wind load which includes drag force $F_y(\alpha)$, lift force $F_z(\alpha)$ and pitch moment $M(\alpha)$.

To solve the nonlinear Eq. (2), an incremental-two-iterative solution scheme is used in this paper. In the inner cycle of iteration, nonlinear analysis of structure under any given wind velocity is carried out using Newton- Raphon method. Nonlinear analysis under the additional wind forces, induced by torsional deformations of the deck that in turn increase wind angles of attack, is performed in the outer cycle of iteration. The use of incremental method is to obtain the wind velocity-deflection curve for a nonlinear aerostatic stability problem. The procedure of calculating critical wind velocity by this scheme can be summarized as follows:

1. Assume an initial wind velocity V_0 ;
2. Calculate wind load of the structure under V_0 ;
3. Solve the global equilibrium Eq. (2) to get the displacement $\{u\}$ by Newton-Raphon method ;
4. Get the torsional angle of element from the displacement $\{u\}$ by averaging the torsional displacement between left node and right node ;
5. Recalculate wind load of the structure under V_0 ;
6. Check if the Euclidean norm of static aerodynamic coefficients is less than the prescribed tolerance. The Euclidean norm is written as:

$$\left\{ \frac{\sum_{j=1}^{Na} [C_k(\alpha_j) - C_k(\alpha_{j-1})]^2}{\sum_{j=1}^{Na} [C_k(\alpha_{j-1})]^2} \right\}^{1/2} \leq \varepsilon_k \quad (k=y,\, z,\, M) \tag{3}$$

   where ε_k=prescribed tolerance; Na=number of nodes subjected to the displacement-dependent wind loads.

   If satisfied, then add wind velocity according to scheduled change in wind velocity length. Otherwise repeat steps (3)-(6) until Eq. (3) is satisfied or the maximum number of iterations is reached.
7. If the iterations do not converge under certain wind velocity, then get back previous wind velocity and recalculate by shortening change length of wind velocity until the difference between two successive wind velocity is less than prescribed tolerance.

4. NASAB software

4.1. Overview

To investigate the nonlinear aerostatic stability of cable-supported bridges, a finite element software, NASAB, was developed. This software has the following capabilities: linear analysis capability, geometric nonlinear analysis capability, material nonlinear analysis capability and nonlinear aerostatic stability analysis capability. For the sake of simplicity, only nonlinear aerostatic stability analysis capability of the software is briefly described in this section. For the interested reader, completed and detailed descriptions of the software can be found in Cheng (2000).

Cable-supported bridges are cable-stayed and suspension bridges. The major structural components of such bridges are the cables (hangers), the towers and the girders (bridge decks). The finite element modeling of these components can be accomplished with the aid of three basic elements: truss element, cable element and beam element. Therefore, the element library used in this software consists of the three elements. The element stiffness matrix, for space truss and space

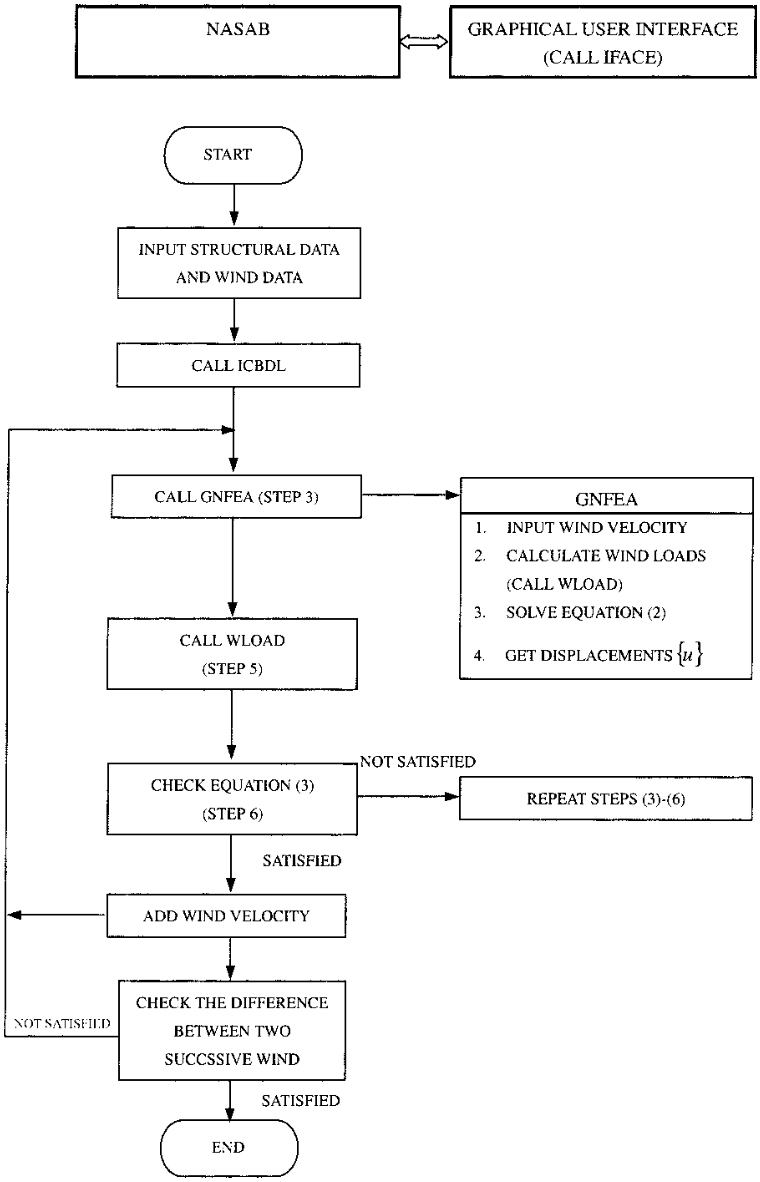

Fig. 2 Flowchart of the NASAB software for the nonlinear aerostatic stability analysis of cable-supported bridges

beam elements, is readily available in Yang, *et al.* (1994) and Boonyapinyo, *et al.* (1994). The cable element and its derived procedure can also available in Karoumi (1999).

The NASAB software was developed using the FORTRAN 77/90 computer language. The use of FORTRAN 77 is to effectively take advantage of existing codes, thus speeding up code design and implementation. FORTRAN90 was used mainly to present the software in a user-friendly environment. Fig. 2 shows the flowchart of the NASAB software for the nonlinear aerostatic stability analysis of cable-supported bridges. The software includes the following main steps (sub-

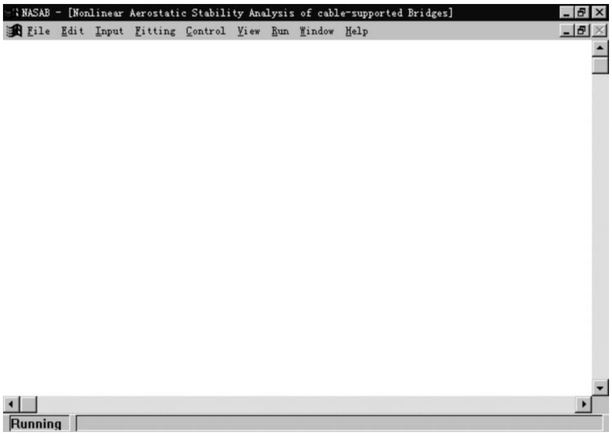

Fig. 3 Graphical user interface of the NASAB software

programs):

1. ICBDL program, which determines the initial configurations of cable-supported bridges under dead loads. The initial configurations are analyzed using a successive substitution method (Wang, *et al*. 1993, Kim and Lee 2001). In this method, the equilibrium equation of a cable-supported bridge is solved iteratively with an assumed tension of each cable element (Kim and Lee 2001).
2. GNFEA program, which performs geometric nonlinear analysis of cable-supported bridges. The co-rotational (CR) formulation (Hsiao, *et al*. 1987) is applied in the formulation of the incremental matrix equilibrium equation of structural models. An incremental-iterative method based on the Newton-Raphson method is used to solve the nonlinear equations.
3. WLOAD program, which calculate the displacement-dependent wind loads acting on a bridge, according to Eq. (1).
4. IFACE program, which develops a graphical user interface (pre-processing and post-processing). This program was developed under Microsoft FORTRAN PowerStation 4.0. Fig. 3 shows the graphical user interface of the NASAB software.

4.2. Validity

Several numerical examples have been solved and compared with available numerical solutions to establish the reliability of the software (Cheng 2000). Three examples are discussed in this paper.

1. Fig. 4 shows an inclined truss acted on by a concentrated vertical load P at the midpoint C and a tensile force T_0. The pertinent data were: the initial length of the truss was taken to be $L=100$ m, the axial rigidity of $EA=1000$ KN, vertical load $P=52.8374$ KN, tensile force $T_0=71.9208$ KN, inclined angle $\alpha=45^{\circ}$. The displacements at the midpoint C and the member axial force are listed in Table 1. The results are in good agreement with theoretical results obtained from Pan Yong-Ren (1996).
2. The large displacement of a cantilever beam subjected to an end moment, M, as shown in Fig. 5, was investigated by Pan Yong-Ren (1996). The finite-element mesh consists of ten two-node

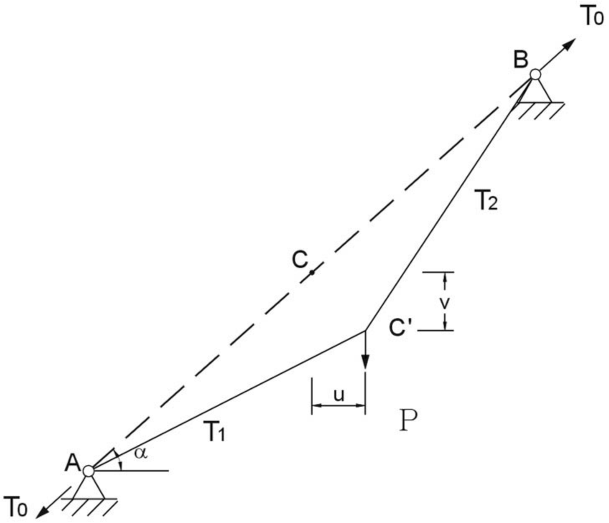

Fig. 4 An inclined truss acted on by a concentrated vertical load P at the midpoint C and a tensile force T_0

Table 1 Results of an inclined truss in Fig. 4

Result obtained from	Displacements (m)		Member axial force (KN)	
	u	v	T_1	T_2
NASAB	6.55988	7.83876	74.9282	112.9220
Pan (1996)	6.55997	7.83885	74.9276	112.9214

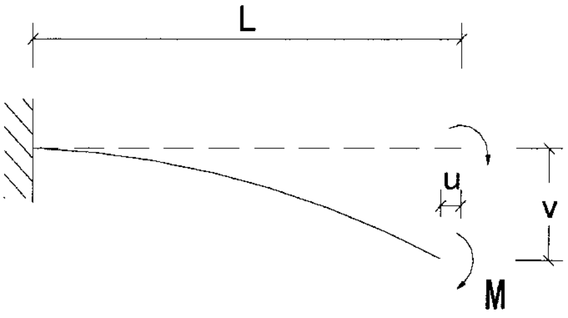

L = 100 m; E = 20.0 MPa; I = 0.08 m^4; A = 0.04 m^2

Fig. 5 Cantilever beam subjected to an end moment

beam element as shown in Fig. 5. The nondimensional displacement parameters V/L and U/L and nondimensional load parameter K, defined as $ML/(2\pi EI)$, where V, U, L are the vertical and horizontal displacements at the free end of the cantilever beam and the length of the cantilever beam, respectively, are listed in Table 2. Good agreement has been observed. Fig. 6 shows deformed configurations of the cantilever beam for different values of K.

Table 2 Results of a cantilever beam in Fig. 5

$K=M\cdot L/2\cdot\pi EI$	V/L		U/L	
	NASAB	Pan (1996)*	NASAB	Pan (1996)*
0.0	0.0	0.0	0.0	0.0
0.2	-0.549664	-0.54987	-0.242946	-0.24317
0.4	-0.719855	-0.71978	-0.765598	-0.76613
0.6	-0.48041	-0.47986	-1.15559	-1.15591
0.8	-0.13803	-0.13747	-1.18947	-1.18921
1.0	-8.37444e-5	0.0	-1.00051	-1.0

Note: * Theoretical solutions from Pan (1996)

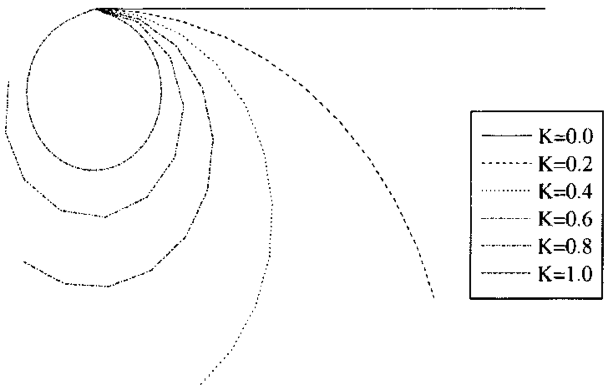

Fig. 6 Deformed configurations of the cantilever beam for different values of K

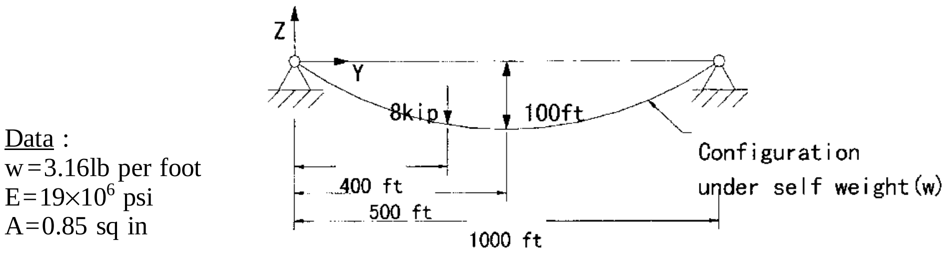

SAG under self-weight at load point : 96.0495 ft

Fig. 7 Isolated cable under concentrated load

3. Fig. 7 shows an isolated cable under concentrated load. The results are compared with that given by Jayaraman and Knudson (1981) and O'Brien and Francis (1964) and Michalos and Birnstiel (1960) as presented in Table 3. From this table, it can be seen that the results obtained by NASAB are quite close to Jayaraman and Knudson' result.

Because this software is accurate, efficient and applicable to aerostatic stability analysis of cable-supported bridges, NASAB has been used extensively in the aerostatic stability analyses of cable-

Table 3 Comparisons of displacements at the load point

Displacement of load point (ft)	NASAB	O'Brien, *et al*. (1964)	Michalos, *et al*. (1960)	Jayaraman, *et al*. (1981)
Vertical	-18.457	-18.460	-17.953	-18.458
Horizontal	-2.8195	-2.820	-2.773	-2.819

supported bridges built in China such as Jiang Yin suspension bridge, Hu Men suspension bridge, 2nd Santou Bay cable-stayed bridge and 2nd NanJing cable-stayed bridge (Cheng 2000).

5. Example

A long-span suspension bridge (Hu Men Bridge) with a main span of 888 m was used to illustrate the aerostatic stability analysis. The reasons for choosing this example bridge are mainly: (1) This bridge is located in Pearl River Estuary region susceptible to high wind speeds; (2) This bridge is symmetrical with respect to the midspan of the bridge. This is different from the asymmetrical suspension bridge described in Cheng, *et al*. (2002).

Fig. 8 shows the general configuration of the bridge. Details concerning the structural parameters of the bridge are omitted for brevity. The interesting reader is referred to Xiang, *et al*. (1994). The effects of wind angle of incidence were not considered. The static aerodynamic coefficients for the bridge studied are shown in Fig. 9 and were incorporated in computer software NASAB by using

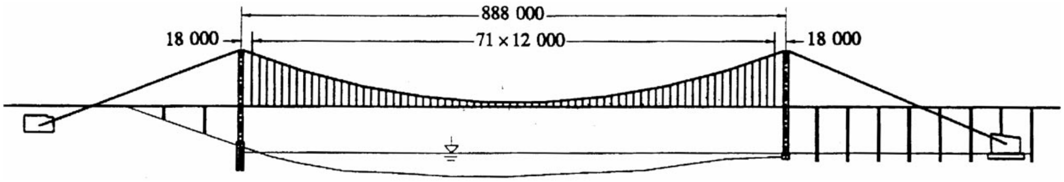

Fig. 8 General configuration of Hu Men Bridge (Unit: mm)

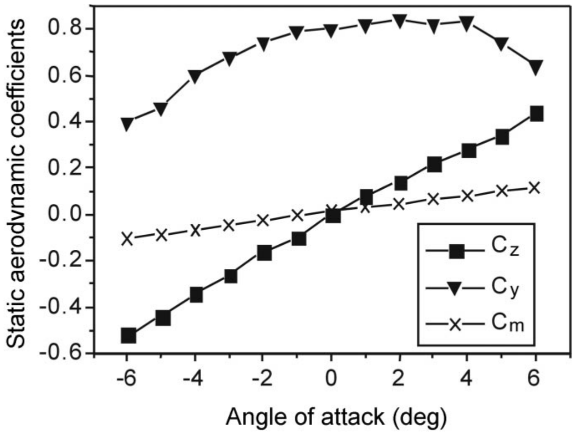

Fig. 9 Static aerodynamic coefficients as Function of Angle of Attack

polynomial function representation. The three components of the displacement-dependent wind loads were only considered for the bridge deck while for the towers and cables only the initial drag force was considered.

5.1. Finite-element modeling

A three-dimensional finite element model has been established for the Hu Men Bridge (Cheng 2000). Three-dimensional beam elements were used to model the two bridge towers. The cables and suspenders were modeled by three-dimensional truss element accounting for geometric nonlinearity due to cable sag. The bridge deck is represented by a single beam and the cross-section properties of the bridge deck are assigned to the beam as equivalent properties. The connections between bridge components and the supports of the bridge were properly modeled.

5.2. Aerostatic stability analysis

Two types of analysis are presented in Table 4: (1) linear aerostatic stability analysis of Xiang, *et al*. (1996); two simplified formulas (see Appendix A and B) are used: one is the torsional divergence formula, and the other is the lateral-torsional buckling formula; (2) nonlinear aerostatic stability analysis using the nonlinear method presented in this paper. From Table 4, it can be seen that: (1) the linear aerostatic stability analysis results in greatly overestimating the critical wind velocity, compared with nonlinear aerostatic stability analysis. The critical wind velocity of 119 m/s obtained from nonlinear aerostatic stability analysis is 13% lower than that of 136 m/s obtained from the linear aerostatic stability analysis based on torsional divergence formula, and is 28% lower than that of 165 m/s obtained from the linear aerostatic stability analysis based on lateral-torsional buckling formula; (2) the critical wind velocity obtained from the linear aerostatic stability analysis based on torsional divergence formula is lower than that obtained from the linear aerostatic stability analysis based on lateral-torsional buckling formula. This indicates that the phenomenon of torsional divergence can occur more frequently than that of lateral-torsional buckling for long span suspension bridges.

Fig. 10 shows torsional, lateral and vertical displacement behaviors at the midpoint of the center span obtained from nonlinear aerostatic stability analysis. Fig. 11 shows instability configuration of the Hu Men Bridge obtained from nonlinear aerostatic stability analysis. From these figures, the following significant characteristics are observed: (1) the displacement responses exhibit strong nonlinearity as the wind velocity increases. This is mainly related to the nonlinearity of three components of displacement-dependent wind loads; (2) the aerostatic instability of the Hu Men Bridge exhibits symmetric flexural-torsional instability in space. However, the aerostatic instability of the Jiang Yin suspension bridge is asymmetric flexural-torsional instability in space (Cheng, *et al*.

Table 4 Comparison of critical wind velocities of the Hu Men Bridge considering different analysis types

Different analysis types	Linear aerostatic stability analysis from (Xiang, *et al*. 1996)		Nonlinear aerostatic stability analysis
	Lateral-torsional buckling	Torsional divergence	
Critical wind velocity (m/s)	165	136	119

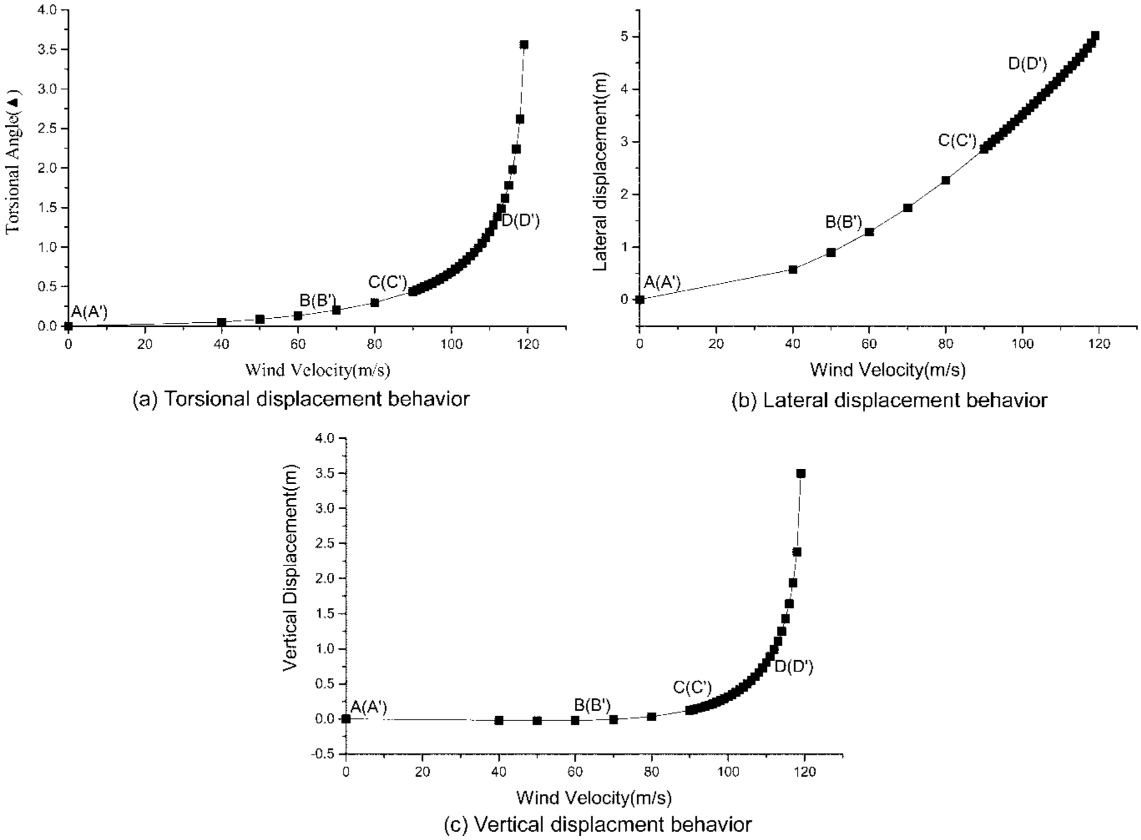

Fig. 10 Displacement behaviors at the midpoint of the center span

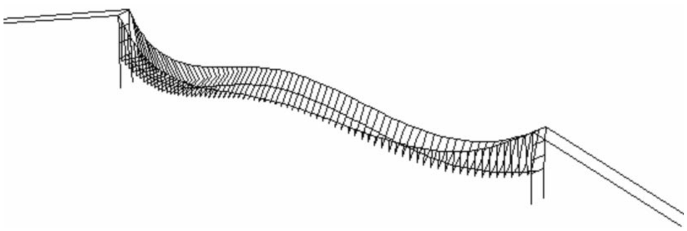

Fig. 11 The instability configuration of the Hu Men Bridge

2002). The difference in the instability configuration between the two suspension bridges may be attributed to the initial configuration (symmetry or asymmetry) of the structures.

6. Aerostatic failure mechanism

Until now the aerostatic failure mechanism of suspension bridges has seldom been studied. In this section, the aerostatic failure mechanism of suspension bridges is explained by tracing aerostatic instability path of the Hu Men Bridge as mentioned above. Fig. 12 shows the tension in uppermost

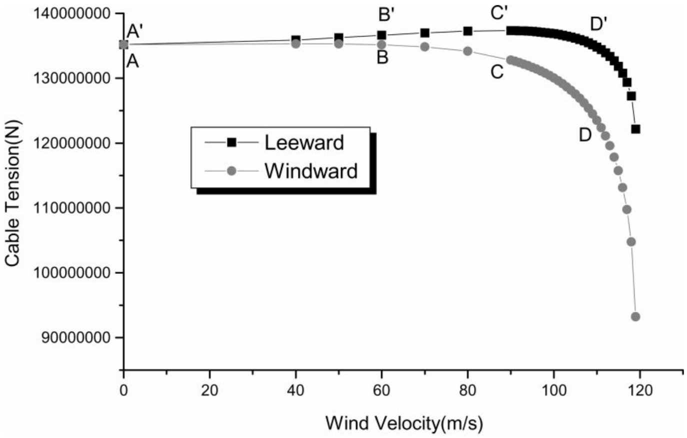

Fig. 12 The tension in uppermost in the center span

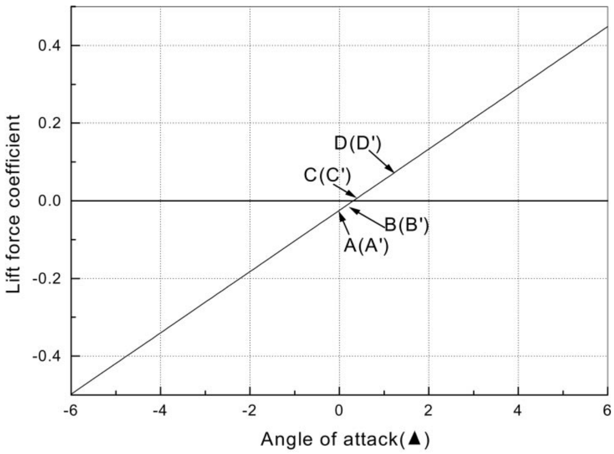

Fig. 13 Lift force coefficient of the Hu Men Bridge

in the center span obtained from nonlinear aerostatic stability analysis. Fig. 13 shows the lift force coefficient of the Hu Men Bridge. A set of deformed configurations of a bridge deck corresponding to locations A (A'), B (B'), C (C') and D (D') as marked in Figs. 10, 12 and 13 are shown in Fig. 14, where O is the center of bridge deck. From Figs. 10, 12-14, it can be seen that the vertical, lateral and torsional displacements of midpoint of center span for the girder are zero at location A (A'). With increasing wind velocity, the vertical, lateral and torsional displacements of midpoint of center span for the girder also increase. At location B (B'), the maximum vertical displacement is obtained. At this time, the lift force coefficient is negative (see Fig. 13). The direction of lift force is downward. At location C (C'), the lift force coefficient becomes positive. The stiffness of structure is lowered by the direction change of lift force. At location D (D'), both the torsional displacement and the in-plane displacements increase remarkably. However, the tensions in cables decrease rapidly. When the wind velocity reaches 119 m/s, the bridge becomes unstable.

Fig. 15 shows the relationship between the resistance forces and wind loads. From this Figure, it can be seen that the nonlinear resistance of the bridge structure decreases as the wind velocity

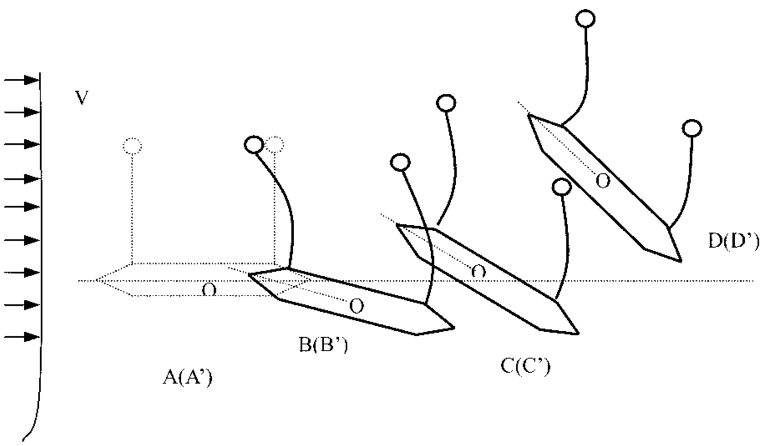

Fig. 14 Deformed configuration of bridge deck at the midpoint of center span

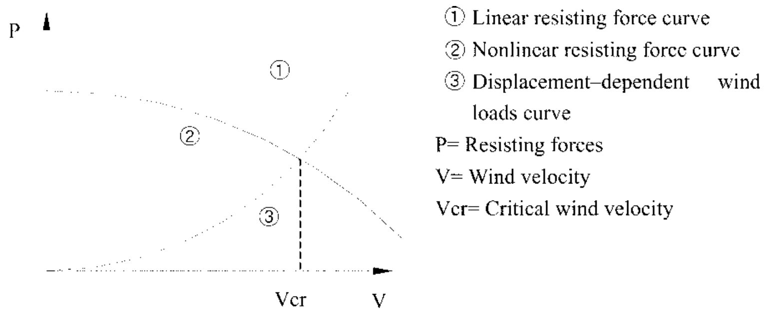

Fig. 15 The relationship between the resistance forces and wind loads

increases. However, the displacement-dependent wind loads acting on the bridge structure increase as the wind velocity increases. When the displacement-dependent wind loads acting on the bridge structure exceed the nonlinear resistance of the bridge structure, aerostatic instability phenomenon takes place.

7. Conclusions

This paper has developed a nonlinear method analyzing the aerostatic behavior of suspension bridges. The method includes the effects of three components of displacement-dependent wind loads and geometric nonlinearity.

The method has been used to investigate the aerostatic stability of suspension bridges. It was found that the linear aerostatic stability analyses of suspension bridges considerably overestimate the critical wind velocity so that they give unsafe results. The actual critical wind velocity should be predicted based on nonlinear aerostatic stability analysis. The initial configuration (symmetry or asymmetry) may affect the instability configuration of structure.

Commercial finite element programs used in civil engineering today cannot be readily used for the aerostatic stability analysis of cable-supported bridges as they lack some capabilities like the calculation of displacement-dependent wind loads, the prediction of critical wind velocity, and determination of initial configurations of cable-supported bridges. The NASAB software appears as a consequence of these necessities. The nonlinear method presented in this research was programmed using the FORTRAN 77/90 computer language and implemented into the software. The software has the following capabilities: linear analysis capability, geometric nonlinear analysis capability, material nonlinear analysis capability and nonlinear aerostatic stability analysis capability. The capabilities and accuracy of the software were examined using various types of practical examples (Cheng 2000). The examples demonstrated that the software yields results, which are consistent with those obtained from exact theoretical or other numerical solutions.

As bridge engineers increasingly consider aerostatic stability of suspension bridges and central span length of suspension bridges becomes longer, investigation on the aerostatic failure mechanism of suspension bridges becomes especially important to be able to accurately understand the aerostatic behavior of suspension bridges. However, study on aerostatic failure mechanism of suspension bridges has not been reported yet. In this paper, the aerostatic failure mechanism of suspension bridges is explained by tracing aerostatic instability path.

Acknowledgments

The writers would like to thank to the National Nature Science Foundation of China under grant number 59895410 for their financial support.

Appendix A. Torsional divergence formula (Xiang, *et al.* 1996)

$$V_{cr} = K_{td} \cdot f_t \cdot B$$

where

$$K_{td} = \sqrt{\frac{\pi^3}{2} \cdot \mu \cdot \left(\frac{r}{b}\right)^2 \cdot \frac{1}{C'_{M0}}}$$

$$\mu = \frac{m}{\pi \rho b^2}, \quad b = \frac{B}{2}$$

$$\frac{r}{b} = \frac{1}{b} \cdot \sqrt{\frac{I_m}{m}}$$

where V_{cr}=critical wind velocity; m=mass per unit length; I_m=mass moment of inertia about the centroidal axis per unit length; ρ is air density; B is bridge width; C'_{M0} is derivative of the pitch moment coefficient at zero angle of attack; f_t=first symmetric torsion frequency.

Appendix B. Lateral-torsional buckling formula (Xiang, *et al.* 1996)

$$V_{cr} = K_{lb} \cdot f_t \cdot B$$

where

$$K_{lb} = \sqrt{\frac{\pi^3 \cdot \left(\frac{B}{H}\right) \cdot \mu \cdot \left(\frac{r}{b}\right)}{C_d \cdot \varepsilon \cdot \sqrt{K} \cdot \sqrt{K + 1 + \frac{C_l' \cdot B_c}{C_d \cdot H}}}}$$

$$K = \frac{1}{4}\left(\frac{4\pi^2}{3} + 1\right) = 3.54$$

$$\varepsilon = \frac{f_t}{f_b}$$

where C_d=drag force coefficient of the stiffened girder; H=the height of the stiffened girder; B_c=width between center lines of cables; C_L' is derivative of the lift coefficient; f_b= first vertical bending frequency.

References

Agar, T.T.A. (1988), "The analysis of aerodynamic flutter of suspension bridges", *Comput. Struct.*, **30**, 593-600.

Agar, T.T.A. (1989), "Aerodynamic flutter analysis of suspension bridges by a modal technique", *Eng. Struct.*, **11**, 75-82.

Booyapinyo, V., Yamada, H. and Miyata, T. (1994), "Wind-Induced nonlinear lateral-torsional buckling of cable-stayed bridges", *J. the Struct. Div., ASCE*, **120**(2), 486-506.

Boonyapinyo, Virote, Miyata, Toshio and Yamada, Hitoshi (1999), "Advanced aerodynamic analysis of suspension bridges by state-space approach", *J. Struct. Eng., ASCE*, **125**(12), 1357-1366.

Cheng, Jin (2000), "Study on nonlinear aerostatic stability of cable-supported bridges", PhD thesis, Tongji University, Shanghai, China (in Chinese).

Cheng, Jin, Jiang Jian-Jing, Xiao Ru-Cheng and Xiang Hai-Fan (2002), "Nonlinear aerostatic stability analysis of Jiang Yin suspension bridge", *Eng. Struct.*, **24**, 773-781.

Hirai, A., Okauchi, I., Ito, M. and Miyata, T. (1967), "Studies on the critical wind velocity for suspension bridges", In: *Proceedings of the international Research Seminar on Wind Effects on Buildings and Structures*. University of Toronto press, Ontario, Canada, 81-103.

Honda, Akihiro, Miyata, Hiroaki, Shibata and Hideyuki (1998), "Aerodynamic stability of narrow decked suspension bridge (Aki-nada Ohashi Bridge)", *J. Wind Eng. Ind. Aerodyn.*, **77&78**, 409-420.

Hsiao, K.M., Horng, H.J. and Chen, Y.R. (1987), "A corotational procedure that handles large rotations of spatial beam structures", *Comput. Struct.*, **27**(6), 769-781.

Jayaraman, H.B. and Knudson, W.C. (1981), "Curved element for the analysis of cable structures", *Comput. Struct.*, **14**(3-4), 325-333.

Karoumi, Raid (1999), "Some modeling aspects in the nonlinear finite element analysis of cable supported bridges", *Comput. Struct.*, **71**, 397-412.

Kim, H.K. and Lee, H.S. (2001), "Analysis of target configurations under dead loads for cable-supported bridges", *Comput. Struct.*, **79**, 2681-2692.

Michalos, J. and Birnstiel, C. (1960), "Movement of a cable due to changed in loading", *J. Struct. Eng., ASCE*, **86**(ST12), 23-38.

O'Brien and Francis, A.J. (1964), "Cable movements under two dimensional loads", *J. Struct. Eng., ASCE*, **90**(ST3), 89-123.

Pan Yong-Ren (1996), "Geometric nonlinear static analysis and construction control of suspension bridges", Ph.D. thesis, Tongji University, Shanghai, China (in Chinese).

Simiu, E. and Scanlan, R. H. (1978), *Wind Effects on Structures - an Introduction to Wind Engineering*, John Wiley and Sons, New York, N.Y.

Wang, P.H., Tseng, T.C. and Yang, C.G. (1993), "Initial shape of cable-stayed bridges", *Comput. Struct.*, **46**(6), 1095-1106.

Xiang, H.F., *et al.* (1994), Key Technology Study for Hu Men suspension bridge, Res. Rep. of Tongji University, Shanghai, China, (in Chinese).

Xiang, H.F, *et al.* (1996), *Wind Resistant Design Guidebook for Highway Bridges*. Beijing: People's Communication Press; (in Chinese).

Xu, Y.L., Sun, D.K., Ko, J.M. and Lin, J.H. (2000), "Fully coupled buffeting analysis of Tsing Ma suspension bridge", *J. Wind Eng. Ind. Aerodyn.*, **85**, 97-117.

Yang, Yeong-Bin and Kuo, Shyh-Rong (1994), *Theory & Analysis of Nonlinear Framed Structures*. Prentice Hall, Singapore.

CC